Submitted to
**Europhysics Conference on High Energy Physics, EPS2007**, July 19-25, 2007, Manchester
Abstract: **200**
Parallel Session: **Physics Beyond the Standard Model**
*Electronic Access: www-h1.desy.de/h1/www/publications/conf/conf_list.html*

# A Search for Excited Neutrinos in $e^-p$ collisions at HERA

H1 Collaboration

**Abstract**

We present a search for excited neutrinos using all $e^-p$ data collected by the H1 experiment at HERA at center-of-mass energy of $318$ GeV with an integrated luminosity of $184$ pb$^{-1}$. The electroweak decay of excited neutrinos, $\nu^* \to \nu\gamma$, $\nu^* \to \nu Z$, $\nu^* \to eW$ are considered and possible final states resulting from the $Z$ or $W$ leptonic and hadronic decays are taken into account. No evidence for excited neutrino production is found. Mass dependent exclusion limits are determined for the ratio of the coupling to the compositeness scale, $f/\Lambda$. These limits extend the excluded region to higher masses than has been possible in previous searches.

# 1 Introduction

The discovery of excited states of quarks or leptons as predicted by compositness models [1, 2] would provide a convincing evidence for a new substructure of matter. Electron-proton interactions at very high energies provide ideal conditions to look for excited states of first generation fermions. In particular a magnetic type coupling of the electron would allow for the production of single excited neutrinos ($\nu^*$) trough t-channel W boson exchange.

In this paper we present a search for excited neutrinos using all $e^-p$ HERA collider data of the H1 experiment. The data collected at electron and proton beam energies of $27.6$ GeV and $920$ GeV respectively corresponds to an integrated luminosity of $184$ pb$^{-1}$. The excited neutrinos are searched for through all their electroweak decays into a fermion and a gauge boson ($\gamma$, $W$ and $Z$). Hadronic decays as well as main leptonic decay channels of the $W$ and $Z$ bosons are considered.

# 2 Phenomenology

Compositeness models [1–4] attempt to explain the hierarchy of masses in the Standard Model by the existence of a substructure within the fermions. Several of these models predict excited states of the known leptons. Excited leptons are assumed to have the same electroweak SU(2) and U(1) gauge couplings, $g$ and $g'$, to the vector bosons, but are expected to be grouped into both left- and right-handed weak isodoublets with vector couplings. The existence of the right-handed doublets is required.

In $ep$ collisions, excited leptons could be produced via the process $ep \to F^* X$ (here X represents the proton remnant or proton in the case of elastic $e^*$ production), as a result of the F*FV couplings. Depending on the details of these couplings, excited leptons could be detected in the photonic, charged current, or neutral current channels.

The branching ratio of the excited leptons into the different vector bosons are determined by the strength of the three F*FV couplings. We use the effective Lagrangian:

$$L_{F^*F} = \frac{1}{2\Lambda}\bar{F}^*_R \sigma^{\mu\nu}[g f \frac{\vec{\tau}}{2}\partial_\mu \vec{W}_\nu + g' f' \frac{Y}{2}\partial_\mu B_\nu]F_L + h.c. \quad (1)$$

which describes the generalised magnetic de-excitation of the excited states. The matrix $\sigma^{\mu\nu}$ is the covariant bilinear tensor, $\tau$ are the Pauli matrices, $W_{\mu\nu}$ and $B_{\mu\nu}$ represent the fully gauge invariant field tensors, and Y is the weak hypercharge. The parameter $\Lambda$ has units of energy and can be regarded as the compositeness scale, while $f$ and $f'$ are the weight associated with the different gauge groups.

The relative values of $f$ and $f'$ also affect the size of the single-production cross-sections and their detection efficiencies. Depending on their relative values, either the photonic decay, the CC decay, or the NC decay will have the largest branching ratio, depending on the respective couplings:

$$f_\gamma = e_f f' + I_{3L}(f - f'), f_W = \frac{f}{\sqrt{2}s_\omega}, f_Z = \frac{4I_{3L}(c^2_\omega f + s^2_\omega f') - 4e_f s^2_\omega f'}{4 s_\omega c_\omega}$$

where $e_f$ is the excited fermion charge, $I_{3L}$ is the weak isospin, and $s_\omega(c_\omega)$ are the sine (cosine) of the Weinberg angle $\theta_\omega$.

Our results for excited neutrinos will be interpreted using the two complementary coupling assignments, $f = f'$ and $f = -f'$. The first uses $f = f'$, so that the photonic decay of the $\nu^*$ is forbidden, the second uses $f = -f'$, so that all $\nu^*$ decays into $\nu\gamma$, $\nu Z$ and $eW$ are allowed.

# 3 Standard Model processes and their simulation

Final states of events selection in this analysis contain either missing transverse momentum or an high energy electron (or photon) and a photon or jets with high tranverse energy. The main backgrounds from Standard Model (SM) processes which could mimic such signatures are mostly neutral current (NC) and charged current (CC) deep-inelastic scattering (DIS) or photoproduction processes. The Born, QCD Compton and Boson Gluon Fusion matrix elements are used in the RAPGAP [5] event generator to model NC DIS and CC DIS events. The QED radiative effects arising from real photon emission from both the incoming and outgoing electrons are simulated using the HERACLES [7] generator. To simulate the direct and resolved photoproduction of jets, prompt photon production and the resolved photoproduction of photon pairs, the PYTHIA $6.1$ event generator [6] is used. Light and heavy flavoured jets are generated. The simulation contains the Born level hard scattering matrix elements and radiative QED corrections. Processes with the production of three or more jets are accounted for using leading logarithmic parton showers as a representation of higher order QCD radiation. Hadronisation is modelled using Lund string fragmentation [6]. The prediction of processes with two or more high transverse momentum jets is scaled by a factor of $1.2$ to normalise the leading order Monte Carlos to next-to-leading order QCD calculations [8]. Contributions from elastic and quasi-elastic QED-Compton scattering are simulated with the WABGEN [9] generator. Possible contributions arising from the production of $W$ bosons or multi-lepton events are also considered and modelled using the EPVEC [10] and GRAPE [11] event generators, respectively.

All generated events are passed through the full GEANT [12] based simulation of the H1 apparatus, which takes into account the running conditions of the different data taking periods.

# 4 The H1 Detector

A detailed description of the H1 experiment can be found in [13]. Only the H1 detector components relevant to the present analysis are briefly described here. Jets and electrons are measured with the Liquid Argon (LAr) calorimeter [14], which covers the polar angle[1] range $4^\circ < \theta < 154^\circ$ with full azimuthal acceptance. Electromagnetic shower energies are measured with a precision of $\sigma(E)/E = 12\%/\sqrt{E/\text{GeV}} \oplus 1\%$ and hadronic energies with

[1]The origin of the H1 coordinate system is the nominal $ep$ interaction point, with the direction of the proton beam defining the positive $z$-axis (forward region). The transverse momenta are measured in the $xy$ plane. The pseudorapidity $\eta$ is related to the polar angle $\theta$ by $\eta = -\ln\tan(\theta/2)$.

$\sigma(E)/E = 50\%/\sqrt{E/\text{GeV}} \oplus 2\%$, as measured in test beams. In the backward region, energy measurements are provided by a lead/scintillating-fiber (SpaCal) calorimeter [15] covering the range $155^\circ < \theta < 178^\circ$. The central and forward tracking detectors are used to measure charged particle trajectories, to reconstruct the interaction vertex and to supplement the measurement of the hadronic energy. The LAr and inner tracking detectors are enclosed in a super-conducting magnetic coil with a strength of $1.15$ T. The luminosity measurement is based on the Bethe-Heitler process $ep \to ep\gamma$, where the photon is detected in a calorimeter located downstream of the interaction point.

# 5 Data Analysis

Events are first selected by requiring that the event vertex be reconstructed within $35$ cm in $z$ of the nominal interaction point. In addition topological filters and timing vetoes are applied to remove background events induced by cosmic showers and other non-$ep$ sources. The main trigger of the events is provided by the LAr calorimeter. The trigger efficiency is close to $100\%$ for events having an electromagnetic deposit in the LAr (electron or photon) with an energy greater than $10$ GeV [16]. For events with missing transverse momentum above $20$ GeV, the trigger efficiency is $\sim 90$ %.

The identification of electrons or photons is first based on the measurement of a compact and isolated electromagnetic shower in the LAr calorimeter. In addition, the electromagnetic cluster is required to be be isolated from jets by a distance $R > 0.5$ to the jet axis in pseudorapidity-azimuth. Energy deposits in the calorimeter and tracks in the inner tracking system are used to form combined cluster-track objects, from which the hadronic energy is reconstructed. Jets are defined using an inclusive $k_T$ algorithm [17, 18] with a minimum transverse momentum of $3$ GeV. The missing transverse momentum $P_T^{miss}$ of the event is derived from all identified particles and energy deposits in the event.

## 5.1 $\nu\gamma$ Resonance Search

For this search, the principal signature is an isolated electromagnetic cluster in events with missing tranverse momentum. Backgrounds arise from CC DIS events with isolated $\pi^0$ or initial or final state radiation. The presence of a neutrino is inferred by requiring $P_T^{miss} > 15$ GeV. A photon is tagged by identifying an electromagnetic cluster with $P_T^\gamma > 20$ GeV in a polar angle range $5^\circ < \theta^\gamma < 120^\circ$. No well measured track should point to the electromagnetic cluster within a distance of closest approach (DCA) of $12$ cm. If $P_T^{miss} < 30$ GeV, thigther vetoes are applied on any charged track pointing to the electromagnetic cluster: no track should be present with a DCA to the cluster below $24$ cm or within $R < 0.5$ in pseudorapidity-azimuth. Radiative CC DIS events are suppressed by requiring that the four-momentum transfer squared determined from the electromagnetic cluster be $\log Q^2_\gamma > 3.5$ GeV$^2$. We also demand that the transverse momentum of the photon be larger that $40$ GeV for events with the variable $\sum_i E^i - P^i_z$ lower than $45$ GeV, where the sum runs over all visible particles. The final state for the signal contains in most of the cases a recoil jet, due to the $\nu^*$ production through a $t$-channel $W$ boson exchange. Hence in the final selection the presence of at least one jet with $P_T^{jet} > 5$ GeV is also imposed.

Nine event survives the selection criteria. The expected SM contribution is $15 \pm 4$ events and is dominated by CC DIS events. The resulting selection efficiency varies from $55\%$ to $40\%$ for excited neutrinos of mass $150$ GeV and $250$ GeV, respectively.

## 5.2 $\nu q\bar{q}$ Resonance Search

For this search, the dominant SM background consists of multi-jet CC DIS events with a moderate contribution from photoproduction. The presence of a neutrino is inferred from substantial missing momentum $P_T^{miss} > 20$ GeV. We use a subsample of events with at least two jets, each having a transverse momentum larger than $20$ and $15$ GeV, respectively, and a polar angle between $5^\circ$ and $130^\circ$. Moreover, the hadron system must exhibit a large polar angle, $\gamma_h > 20^\circ$, in order to remove photoproduction events. At low $P_T^{miss}$, cuts on the variable $\sum_i E^i - P_z^i$ and on the ratio $V_{ap}/V_p$ of transverse energy flow anti-parallel and parallel to the hadronic final state [16] are used to suppress CC DIS events. In events with $P_T^{miss} < 30$ GeV, we require $V_{ap}/V_p > 0.1$ and in addition if $P_T^{miss} < 50$ GeV events with $\sum_i E^i - P_z^i < 25$ GeV are removed. Finally, to further suppress the background from CC DIS a cut on the jet multiplicity ($n_{jets} \geq 3$) is applied in the region of lower missing transverse momentum ($P_T^{miss} < 50$ GeV). The $Z$ candidate is reconstructed from the combinaison of two jets with an invariant mass closest to the nominal $Z$ boson mass. The reconstructed mass is required to be above $60$ GeV. After these cuts, $111$ events are found compared to an expected SM contribution of $102 \pm 24$ events. No significant excess is observed. The acceptance for $\nu^*$ events in this final state is approximately $40$ % for $M_{\nu^*} > 150$ GeV.

## 5.3 e$q\bar{q}$ Resonance Search

In this channel multi-jet NC DIS events constitute the main contribution from SM processes. Events are selected by the presence of an electron in the LAr ($5^\circ < \theta^e < 90^\circ$) with $Q_e^2 > 2500$ GeV$^2$ or a tranverse momentum $P_T^e$ greater than 25 GeV. The restriction on the electron polar angle to the forward region of the LAr removes a large part of the NC DIS contribution. The presence of at least two high $P_T$ jets with $P_T^{jet1,\,jet2} > 20, 15$ GeV and $5^\circ < \theta^{jet1,\,jet2} < 130^\circ$ is required. Then, a $W$ candidate is reconstructed in those events from the combinaison of two jets with an invariant mass closest to the nominal $W$ boson mass. The reconstructed mass of the $W$ candidate is required to be larger than $40$ GeV. To increase the separation power between NC DIS events and a $\nu^*$ signal we demand that the polar angle of the higest $P_T$ jet associated to the $W$ candidate be lower than $80^\circ$ and that the events with $P_T^e < 65$ GeV contain at least three jets. After the selection, $198$ events are observed while $189 \pm 33$ are expected from the SM. The efficiency for selecting $\nu^*$ events varies between 30–40 % in this decay channel.

## 5.4 Resonance Search in leptonic decays of $W$ and $Z$ bosons

In the search for $\nu^* \rightarrow eW_{\hookrightarrow \nu\mu}$ events with a $P_T^{miss} > 12$ GeV and one isolated electron and muon are selected. The electron and muon have to be isolated and to verify $P_T^{e,\mu} > 20, 10$ GeV and

$\theta_{e,\mu} < 100^\circ, 160^\circ$. After this selection no data event is left while $0.54 \pm 0.04$ SM background events are expected.

The signature for the $\nu^* \to eW_{\hookrightarrow \nu e}$ and $\nu^* \to \nu Z_{\hookrightarrow ee}$ channels is similar and consist of two high $P_T$ electrons and a large missing transverse momentum, $P_T^{miss} > 20$ GeV. Two isolated electromagnetic clusters are first required, with a transverse momentum larger than $20$ and $15$ GeV and a polar angle $5^\circ < \theta_{e1,e2} < 100^\circ, 120^\circ$, respectively. To reduce background from Compton events, a track of any quality has to be associated to each electromagnetic cluster in the central region ($\theta_e > 35^\circ$). Events from the $W_{\hookrightarrow \nu e}$ decay channel are selected by imposing the invariant mass of the $\nu$ and the electromagnetic cluster to be compatible with the $W$ boson mass within $20$ GeV. Events in which the invariant mass of the two electromagnetic clusters is close to the mass of the $Z$ boson by $10$ GeV are attributed to the $Z_{\hookrightarrow ee}$ decay channel. No candidate is found in both channels, compared to SM expectations of $0.6 \pm 0.3$ and $0.12 \pm 0.04$ in the $W$ and $Z$ decay channels, respectively.

# 6 Interpretation

The event yields observed in each decay channel are summarised in table 1. The observed event yields are in good agreement with SM expectations, which are dominated by NC DIS for $eq\bar{q}$ resonance search and by CC DIS events for $\nu\gamma$ and $\nu q\bar{q}$ resonance searches. The distributions of the invariant mass of the data events and of expected SM background are compared in figure 1 for the main three channels. Both data and SM are in agreement and no additional resonance is seen in the data. No data events is observed in channels corresponding to leptonic decays of $W$ or $Z$ bosons in agreement with SM expectations below one in those classes.

Since there is no evidence for excited neutrinos, upper limits on the coupling $f/\Lambda$ as a function of the mass of the excited neutrino are derived. Limits are presented at the 95 % confidence level and are obtained using a modified frequentist approach [19] which takes statistical and systematical uncertainties into account.

The resulting limits after combination of all decay channels are presented in figure 2, for the conventional assumptions $f = -f'$ and $f = +f'$. Note that the decay $\nu^* \to \nu\gamma$ is forbidden for $f = +f'$. This new result improve significantly the bounds previously obtained by H1 [20] using 15 pb$^{-1}$ of HERA I data and extend up to the HERA kinematical limit. Considering the assumption $f/\Lambda = 1/M_{\nu^*}$ excited neutrinos with masses up to 211 GeV (195 GeV) are excluded for $f = -f'$ ($f = +f'$).

For comparisons, results obtained in $e^+e^-$ collisions at LEP by the L3 collaboration [21] are also shown on figure 2. The limits from the present analysis are more stringent at high masses and extend beyond the kinematic reach of previous searches.

# 7 Summary

In summary, using all $e^-p$ data collected by the H1 experiment with an integrated luminosity of 184 pb$^{-1}$ a search for the production of excited neutrinos has been performed. The excited

neutrino decay channels $\nu^* \to \nu\gamma$, $\nu^* \to \nu Z$ and $\nu^* \to eW$ with subsequent hadronic or leptonic decays of the $W$ and $Z$ bosons have been considered and no indication of a signal was found. New limits on the coupling $f/\Lambda$ as a function of the excited neutrino masses have been established, using the two specific relations between the couplings $f = f'$ and $f = -f'$. Assuming $f = -f'$ and $f/\Lambda = 1/M_{\nu^*}$ excited neutrinos with a mass lower than 211 GeV are excluded at 95% confidence level. The present results greatly extend previous searched domains at HERA and confirm the HERA unique sensitivity for excited neutrinos with masses beyond the LEP reach.

# References


[1] H. Harari, Phys. Rept. **104** (1984) 159.

[2] F. Boudjema, A. Djouadi and J. L. Kneur, Z. Phys. C **57** (1993) 425.

[3] K. Hagiwara, D. Zeppenfeld and S. Komamiya, Z. Phys. C **29** (1985) 115.

[4] U. Baur, M. Spira and P. M. Zerwas, Phys. Rev. D **42** (1990) 815.

[5] H. Jung, Comput. Phys. Commun. **86** (1995) 147.

[6] T. Sjostrand, P. Eden, C. Friberg, L. Lonnblad, G. Miu, S. Mrenna and E. Norrbin, Comput. Phys. Commun. **135** (2001) 238, [hep-ph/0010017].

[7] A. Kwiatkowski, H. Spiesberger and H. J. Mohring, Comput. Phys. Commun. **69** (1992) 155.

[8] C. Adloff *et al.* [H1 Collaboration], Eur. Phys. J. C **25** (2002) 13, [hep-ex/0201006].

[9] C. Berger and P. Kandel, Prepared for Workshop on Monte Carlo Generators for HERA Physics Hamburg, Germany, 27-30 Apr 1998.

[10] U. Baur, J. A. Vermaseren and D. Zeppenfeld, Nucl. Phys. B **375** (1992) 3.

[11] T. Abe, Comput. Phys. Commun. **136** (2001) 126, [hep-ph/0012029].

[12] R. Brun, F. Bruyant, M. Maire, A. C. McPherson and P. Zanarini, CERN-DD/EE/84-1.

[13] I. Abt *et al.* [H1 Collaboration], Nucl. Instrum. Meth. A **386** (1997) 310 and 348.

[14] B. Andrieu *et al.* [H1 Calorimeter Group Collaboration], Nucl. Instrum. Meth. A **336** (1993) 460.

[15] R. D. Appuhn *et al.* [H1 SPACAL Group Collaboration], Nucl. Instrum. Meth. A **386** (1997) 397.

[16] C. Adloff *et al.* [H1 Collaboration], Eur. Phys. J. C **30**, 1 (2003), [hep-ex/0304003].

[17] S. D. Ellis and D. E. Soper, Phys. Rev. D **48** (1993) 3160 [hep-ph/9305266].

[18] S. Catani, Y. L. Dokshitzer, M. H. Seymour and B. R. Webber, Nucl. Phys. B **406** (1993) 187.

[19] T. Junk, Nucl. Instrum. Meth. A **434** (1999) 435, [hep-ex/9902006].

[20] C. Adloff *et al.* [H1 Collaboration], Phys. Lett. B **525** (2002) 9, [hep-ex/0110037].

[21] M. Acciarri *et al.* [L3 Collaboration], Phys. Lett. **B 502** (2001) 37, [hep-ex/0011068].

Search for $\nu^*$, HERA I+II ($e^-p$, 184 pb$^{-1}$, preliminary)

| Selection | Data | SM | Efficiency $\times$ BR |
|---|---|---|---|
| $\nu^* \to \nu\gamma$ | 9 | $15 \pm 4$ | 50 % |
| $\nu^* \to eW_{\hookrightarrow qq}$ | 198 | $189 \pm 33$ | 30–40 % |
| $\nu^* \to \nu Z_{\hookrightarrow qq}$ | 111 | $102 \pm 24$ | 40 % |
| $\nu^* \to eW_{\hookrightarrow \nu\mu}$ | 0 | $0.54 \pm 0.04$ | 3–4.5 % |
| $\nu^* \to eW_{\hookrightarrow \nu e}$ | 0 | $0.6 \pm 0.3$ | 4–6 % |
| $\nu^* \to \nu Z_{\hookrightarrow ee}$ | 0 | $0.12 \pm 0.04$ | 2 % |

Table 1: Observed and predicted event yields for the studied decay channels. The analysed data sample corresponds to an integrated luminosity of 184 pb$^{-1}$. The errors on the prediction include model uncertainties and experimental systematic errors added in quadrature.

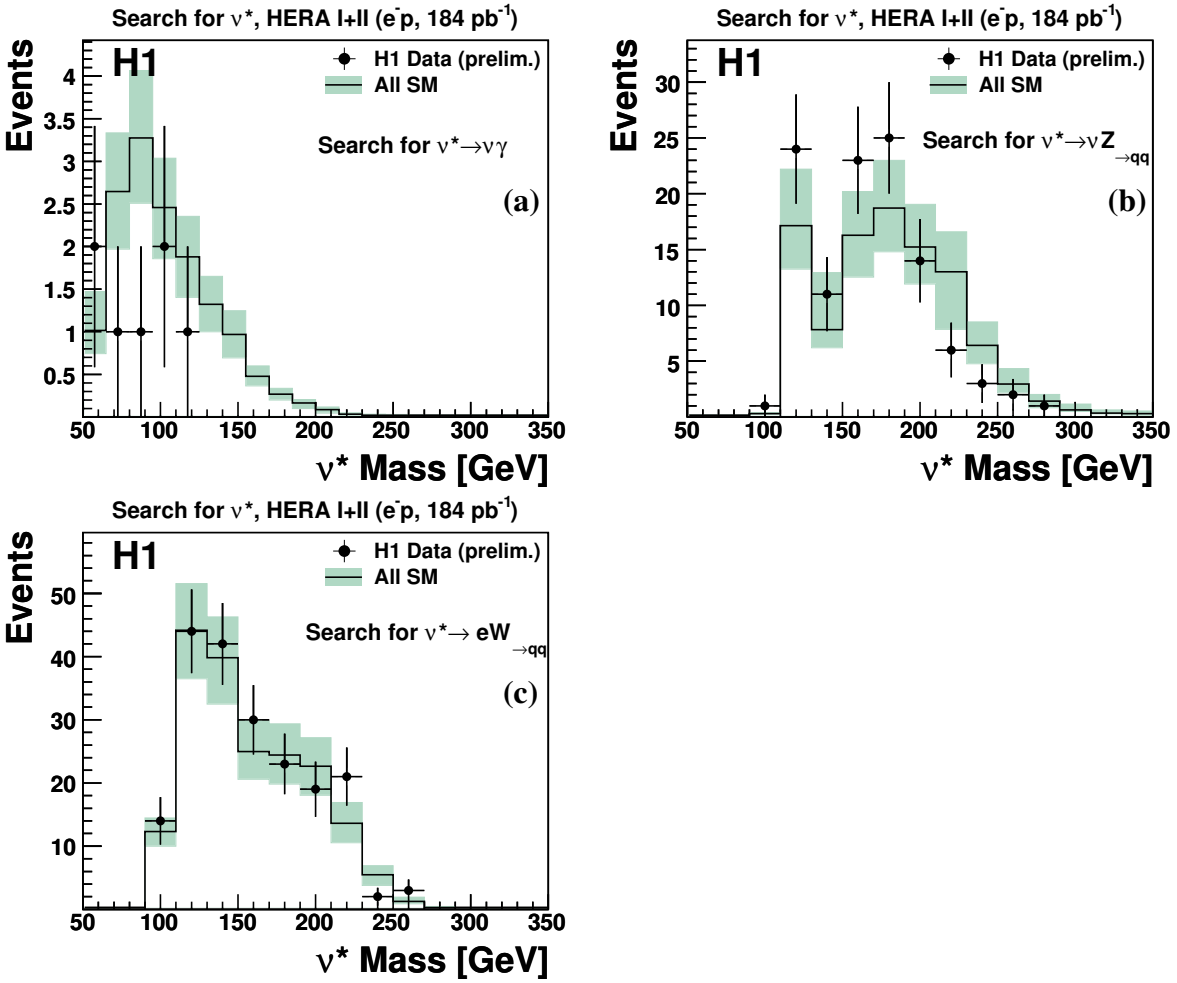


Figure 1: Invariant mass distribution of the $\nu^*$ candidates for the (a) $\nu^* \to \nu\gamma$, (b) $\nu^* \to \nu Z_{\hookrightarrow q\bar{q}}$ and (c) $\nu^* \to eW_{\hookrightarrow q\bar{q}}$ searches. The points corresponds to the observed data events in the final selections and the histogram to the total SM prediction. The error bands on the SM prediction include model uncertainties and experimental systematic errors added in quadrature.

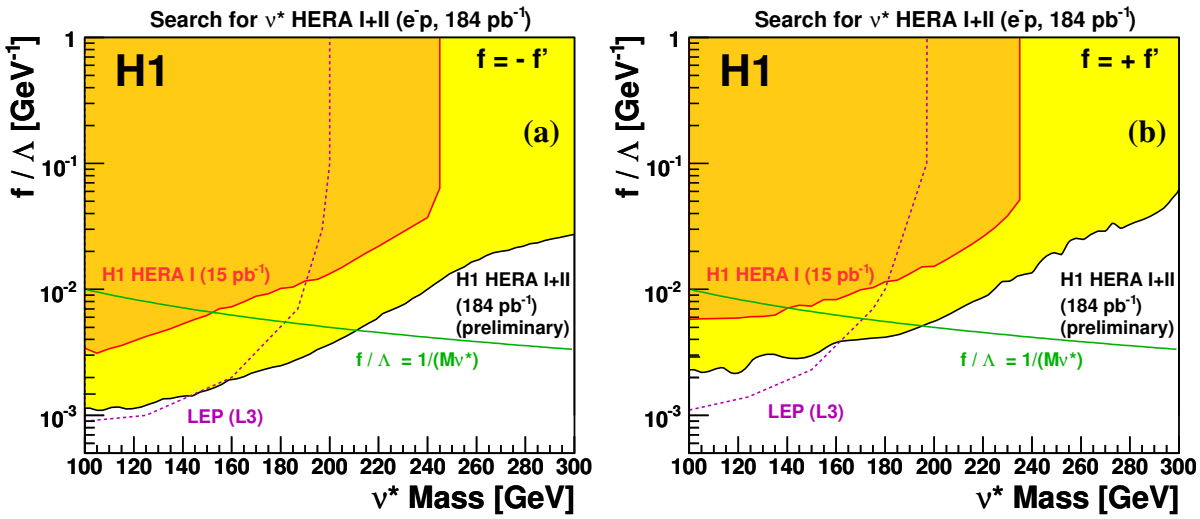


Figure 2: Exclusion limits on the coupling $f/\Lambda$ at 95% C.L. as a function of the mass of the excited neutrino with the assumptions (a) $f = -f'$ and (b) $f = +f'$. The observed limits from this analysis using all H1 $e^- p$ data is represented by the yellow area. Values of the couplings above the curves are excluded. The orange-dark area corresponds to the exclusion domain published by the H1 experiment [20] using 98/99 data and the dashed line to the exclusion limit from the L3 experiment at LEP [21].